

Pressure-Sensitive Paint Measurements on Surfaces with Non-Uniform Temperature

Timothy J. Bencic
NASA Lewis Research Center
Cleveland, OH 44135

Keywords

Pressure-sensitive paint, Temperature-sensitive paint, Pressure measurement, Luminescent quenching, Surface measurement

Abstract

Pressure-sensitive paint (PSP) has become a useful tool to augment conventional pressure taps in measuring the surface pressure distribution of aerodynamic components in wind tunnel testing. While the PSP offers the advantage of a non-intrusive global mapping of the surface pressure, one prominent drawback to the accuracy of this technique is the inherent temperature sensitivity of the coating's luminescent intensity. A typical aerodynamic surface PSP test has relied on the coated surface to be both spatially and temporally isothermal, along with conventional instrumentation for an *in situ* calibration to generate the highest accuracy pressure mappings. In some tests however, spatial and temporal thermal gradients are generated by the nature of the test as in a blowing jet impinging on a surface. In these cases, the temperature variations on the painted surface must be accounted for in order to yield high accuracy and reliable data. A new temperature correction technique was developed at NASA Lewis to collapse a "family" of PSP calibration curves to a single intensity ratio versus pressure curve. This correction allows a streamlined procedure to be followed whether or not temperature information is used in the data reduction of the PSP. This paper explores the use of conventional instrumentation such as thermocouples and pressure taps along with temperature-sensitive paint (TSP) to correct for the thermal gradients that exist in aeropropulsion PSP tests. Temperature corrected PSP measurements for both a supersonic mixer ejector and jet cavity interaction tests are presented.

Introduction

Global measurement techniques have dramatically increased the amount of information realized during a wind tunnel test compared to point measurements. The additional information leads to an increased understanding of the flow physics around an aerospace vehicle thus decreasing its design cycle time. One of these widely accepted techniques is the measurement of surface pressures using pressure-sensitive paints¹⁻³. These paints are comprised of a luminescent compound (luminophore) or dye that is quenched by oxygen and is dispersed in an oxygen permeable polymeric binder. The luminescence is induced by the excitation of the dye at its absorption wavelength. The emitted intensity of the PSP is inversely proportional to the partial pressure of oxygen.

The relationship between the intensity of the luminescence and the partial pressure of oxygen can be expressed in terms of the Stern Volmer relation given by

$$\frac{I_0}{I_{O_2}} = 1 + K_{SV} P_{O_2} \quad (1)$$

where:

P_{O_2} = Partial pressure of oxygen

I_0 = luminescent intensity at zero oxygen pressure

I_{O_2} = luminescent intensity at partial pressure of oxygen P_{O_2}

K_{SV} = Stern Volmer constant

In general it is not practical or even feasible to measure I_0 in a wind tunnel environment. By using Henry's Law that linearly relates the ambient pressure P to the partial pressure of oxygen in air, equation 1 can be rewritten using the popular intensity ratio based form

$$\frac{P}{P_{REF}} = A + B \frac{I_{REF}}{I} \quad (2)$$

where:

I_{REF} = "wind-off" intensity at constant pressure P_{REF}

I = "wind-on" intensity at pressure P

It should be noted that both A and B in equation 2 are temperature dependent. A more detailed derivation of these equations and the corresponding equations for TSP is well documented⁴⁻⁶ and will not be presented in this paper.

The intensity technique requires two data points to be acquired, I_{REF} and I , to determine the unknown pressure P . The technique holds true whether the acquired intensity data is from a single point detector or two dimensional intensities from a CCD camera. Since all the data used in this paper were acquired with a cooled CCD camera, the data points will be referred to as images. The reference image is acquired at a constant known pressure usually at ambient conditions, and is commonly referred to as the "wind-off" image. The image of the unknown pressure at test conditions is referred to as the "wind-on" image.

Photoluminescence is a radiative process that occurs when a luminescent molecule is stimulated by the absorption of light. When the molecule absorbs a photon, it can be excited to a higher energy state. From this excited state, the luminescence process competes with non-radiative processes such as oxygen quenching to return the excited molecule to the initial ground state. The energy change for absorption is greater than for the emission process. Utilizing Einstein's relationship between wavelength and energy transition, the mean wavelength for absorption is shorter than the mean wavelength of emission. The separation of the excitation and emitted light allows the two signals to be spectrally separated and allows the emitted light to be recorded. It is essential that the camera record only the emission spectra. Therefore the excitation must be filtered sufficiently so that it emits no light in the emission band. Similarly, the detection system must be filtered to ensure the camera only records the emission band of the PSP.

There are three main sources of error using the intensity based PSP technique. The first type of error is from the physical and chemical properties of the paint. These include but are not limited to the temperature sensitivity, induction effects, photodegradation and moisture sensitivity of the paint. There are two major factors that constitute the temperature dependence of a PSP. They are the temperature dependence of the emission quantum yield of the luminophore and the dependence of the binder's oxygen permeability. The quantum yield or the amount of absorbed and emitted light by the luminophore is the fundamental principle of the luminescence process as described above. The quenching of the luminophore depends on the diffusivity and solubility of oxygen in the paint binder. This changes as the temperature of the paint binder changes and dictates the amount and transport speed of the oxygen through the binder to the luminescent molecules. The second type is the measurement system errors from the equipment used in the technique. Samples of these errors are temporal variation in the excitation light source; errors associated with the photodetector (dark current, readout noise, etc.), excitation and emission filter overlap and stray light. The third type of error source has to do with the actual test article. The deformation and displacement of the test article between the "wind-off" and "wind-on" images leads to a non-repeatable excitation light field and registration inaccuracies. These effects are also complicated for tests that require multiple runs to acquire both pressure and temperature data. The model geometry can also lead to reflections, shadowing and self-illumination. The technique to be presented here addresses the first type of errors discussed above, minimizing the errors associated with temperature gradients on the painted test article.

As stated earlier, the intensity based PSP technique requires two images, a wind-off reference image and a wind-on data image to determine the unknown pressure distribution of the test data image. In a similar fashion, the intensity based TSP techniques requires the same two images. Figure 1 shows the data reductions steps required to produce quantitative pressure distributions. Scientific grade CCD cameras are precision instruments to measure light but need corrections to minimize pixel to pixel variations in sensitivity and zero offset. These corrections are made using dark and flat-field images. A dark image is an image with no light incident on the CCD and records the bias or offset of the CCD and electronics. A flat-field image is an image of a uniformly lighted surface and record each pixels sensitivity to a given intensity of light. All wind-on and wind-off images are corrected for the cameras CCD sensitivity and offsets. When using the temperature data from the TSP to correct the PSP, all four images must be spatially aligned to sub-pixel accuracy for a true representation of the surface pressure and temperature. After the alignment, the wind-off reference is divided by the wind-on image. This ratio utilizes the constant pressure reference to normalize the data image for non-uniformities in paint application and excitation illumination.

There are two methods of calibrating the intensity ratios once they have been established. The first technique utilizes a-priori information from a sample painted at the same or prior time and calibrated in a calibration chamber. The second method referred to as an in-situ calibration relies on conventional instrumentation on the test article such as pressure transducers and thermocouples to generate the paint's calibration. The conventional instrumentation and intensity ratio data are used to generate a least square error curve fit to generate a calibration for all pixels on the test article. Combinations of both calibration methods are typically used in tests at NASA Lewis. The a priori calibration is first applied as a second order curve fit to the intensity ratio to give a pressure or temperature image. Then the in-situ calibration is applied as a linear correction utilizing information from instrumentation on the test article. Once the temperature image has been determined, the temperature dependence of the PSP intensity ratio is

corrected using the a priori calibration. The temperature corrected PSP intensity ratio is then calibrated using the a priori and in-situ calibrations to produce the final pressure distribution images.

Temperature Corrections

PSP tests have been performed at the NASA Lewis Research Center on articles made of many types of materials. These materials range from good thermal conductors such as copper, aluminum, steel, stainless steel and titanium to materials that are less thermally conductive such as glass, acrylic sheet, carbon fiber composites and stereo-lithography constructed models. Also, since we primarily perform propulsion component tests at Lewis, our experiments tend to have a higher degree of thermal variation than other types of aerodynamic testing. Tests routinely have high-speed jets of air impinging on the painted surfaces, or rotating machinery components that inherently have temperature gradients. An ideal PSP would have a high sensitivity to pressure and no or minimal change in luminescent intensity due to temperature to eliminate the inherent thermal effects of these tests. The ideal paint does not exist, and therefore the thermal effects must be accounted for. These non-isothermal tests require a systematic approach to the data reduction procedure.

A typical calibration of pressure versus intensity ratio at different temperatures for a PSP consisting of a Ruthenium complex luminophore in a silicone binder is shown in figure 2. The family of curves uses a reference image at a constant ambient temperature of 21°C and 1 atmosphere that in most PSP tests is approximately the temperature of the "wind-off" reference images. It should also be noted that the calibration curves show that there is a pressure level dependency of the temperature effect on the paint. This shows the temperature dependence of the binder's oxygen permeability and the effects it has on the quenching process through the diffusivity and solubility of oxygen in the binder at different temperatures. It has been shown by Woodmansee et al⁷ that if the intensity ratio and temperature are known at every pixel location, then the pressure may be determined by using an $I_{REF}/I_{CAL} = f(P,T)$ calibration surface. The method explored here goes one step further and assumes that given the intensity ratio and temperature at every pixel, a corrected intensity ratio can be determined that is dependent on temperature only in the form of $[I_{RATIO}]_{COR} = I_{RATIO}\{T\}$ since the intensity ratio is already pressure dependent. This correction would collapse the family of curves of figure 2 down to a single curve at ambient temperature or the 21°C curve.

The calibration data of figure 2 follows the functional form given in equation 3. When equation 3 is applied, the family of calibration curves collapse to a single intensity ratio curve. The corrected intensity ratio equation is

$$\left[\frac{I_{REF}}{I} \right]_{COR} = \frac{I_{REF}}{I} (CT^2 + DT + E) \quad (3)$$

The values C, D and E are determined using a linear least squares fit to the data acquired on sample coupons in a PSP calibration rig. Figure 3 shows the corrected intensity ratio data of figure 2 using equation 3 with values of $C = 1.822 \times 10^{-4}$, $D = -0.1273$, $E = 22.664$ where T is in degrees Kelvin. By collapsing the intensity ratio curves to a single curve, only one equation that determines the pressure with a known intensity ratio is needed rather than a calibration surface. The need for only a single equation relating pressure to intensity ratio makes the data reduction process the same whether the

temperature gradient is known or the data is acquired using a thermally soaked test article which is often the case for wind tunnel PSP testing. Thus far, only the Ruthenium paint used at Lewis has been corrected using this procedure. Future plans are to investigate other paint formulations to see if this correction technique is applicable.

Experimental Results

A reliable spectrally separable dual pressure/temperature sensing paint was not available at the time of testing so single luminophore PSP and TSP coatings were used. This requires each coating to be applied individually to the test article and a separate test run to get the appropriate data. The data reduction procedures used for the temperature corrected PSP uses a combination of a priori and in situ information. Most test articles have limited instrumentation that is used for the in-situ calibration of both the TSP and PSP. The exceptions are rotating surfaces that typically do not have instrumentation and all calibrations must rely purely on a priori information. The temperature sensitivity correction of the PSP always relies on a priori data acquired from sample coupons in a separate calibration cell. The temperature compensation is done on a pixel by pixel basis using equation 3 along with the aligned temperature image and the pressure intensity ratio image. Two experiments are presented from work done at Lewis that illustrate the technique for improved temperature correction of PSP.

The first test is a supersonic multi-jet mixer ejector nozzle test⁸ in which the test article walls are made from acrylic sheet and instrumented with pressure taps and thermocouples. Figure 4 shows the test article, jet locations and the location of the thermocouples and pressure taps. The PSP/TSP equipment used in this experiment is described in Reference 9. Figure 5 shows the temperature gradients that exist for the straight ejector sidewall where the primary jets have a Mach number of 1.39. The complex temperature distribution on the ejector sidewall is clearly evident from the four impinging supersonic jets. In fact, the temperature distribution in the substrate is a low pass version of the pressure field due to the low response time of the thermal diffusivity. The in-situ calibrations of the temperature images were performed using all 15 thermocouples when the painted ejector wall was painted with TSP. The PSP images with and without temperature corrections are shown in figures 6 and 7. Both images were also calibrated using the 15 pressure taps available on the model but due to the complex temperature gradients, the uncorrected images contain significant errors. The PSP image data and the difference between the taps and image data are shown in the Table I for the uncorrected and temperature corrected images using the two different calibration schemes. The image data is an average of a five by five pixel area centered around its associated pressure tap.

In this experiment, the temperature correction provided very good pressure data results. The a priori calibration after the temperature compensation was applied to the PSP had a rms error of 2.66 kPa. Woodmansee and Dutton suggest in a similar type of experiment that an in-situ calibration is the preferred procedure to obtain the highest accuracy surface pressure measurements. However, the data in Table I suggests that in experiments with high temperature gradients, it is more important to temperature correct the data than to fit the image data to the pressure taps. In fact, the temperature corrected a priori calibration is a more accurate measurement as shown by the rms error values than the non-temperature corrected in-situ since it better represents the lower pressure near the jet exit and higher pressure at the

ejector exit. Further analysis of the data shows that using in-situ information, when available, is the preferred method as concluded by Woodmansee.

The second experiment is the steady state surface pressure distribution produced by a jet-cavity interaction¹⁰. Flows over cavities exhibit significant changes in the steady and unsteady pressure fields that are of critical importance to aerospace applications. Flows over cavities occur in aircraft wheel wells, in-flight refueling ports, weapons bays as well as a significant number of other applications. Thus far, only the steady state surface pressure fields have been studied using PSP. The test article was constructed of aluminum, which has significantly different thermal properties than the clear acrylic used in the previous example. The rectangular cavity dimensions were 4.5 cm wide, 10.2 cm long and 1.3 cm deep. The cavity was attached to the exit of the jet nozzle thus providing the flow stream over the cavity. The instrumentation was sparse comprised of only three pressure and three thermocouples on the floor of the cavity. Similar to the mixer ejector case, the PSP and TSP measurements were made in sequential tests. The temperature and pressure profiles are shown in figures 8 and 9 for a left to right jet velocity of Mach 1.02. It should be noted that the temperature gradients are not as severe as those in the previous example. One would expect the accuracy of a linear in-situ calibration for the non-temperature compensated data to be very good. In this case the rms error between the pressure taps and the pressure image data is 1.78 kPa and outperforms a temperature compensated a priori calibration by almost a factor of two. However, by correcting the data for temperature gradients and using a linear in-situ calibration, the error can be cut in half to 0.86 kPa. The plot in figure 10 shows the two in-situ calibrated pressure images and how the temperature correction effects the PSP data as the temperature gradient increases.

Conclusion

The ideal PSP, if it were to exist, would be insensitive to temperature, but since this is not the case, one must account for the temperature distribution of the surface of a test article. A temperature correction routine has been developed that takes a family of pressure versus intensity ratio curves and collapses them to a single curve. The advantage of using this type of data reduction method is that a single pressure/intensity ratio calibration holds true for all corrected intensity ratio images. The one remaining type 1 item that significantly contributes to the error of these measurements is the lack of a reliable dual pressure and temperature luminophore paint. The repeatability of article assembly and test conditions limits the accuracy of the acquired data for single probe paints.

The mixer-ejector nozzle test shows that combining the use of conventional pressure and temperature sensors with PSP and TSP can minimize the impact of large temperature gradients on the measured pressure. Using a priori calibration information actually yielded a lower error between the pressure taps and image data than an in-situ calibration which used all available pressure taps in the calibration. The temperature corrected pressure images of the jet cavity interaction test reduced the error by a factor of two. This indicates that the accuracy of a PSP measurement can be increased when temperature gradients are accounted for not only on low thermally conductive materials such as the acrylic but also high thermal conductivity materials such as aluminum.

Table I. Mixer Ejector pressure tap and PSP image data comparison.

| Pressure in kPa | Non-compensated | | | | Temperature Corrected | | | | |
|--------------------|----------------------|-------|---------------------|-------|-----------------------|-------|---------------------|-------|-------------|
| | a priori calibration | | in-situ calibration | | a priori calibration | | in-situ calibration | | |
| Tap # | Tap | Image | (Tap-Image) | Image | (Tap-Image) | Image | (Tap-Image) | Image | (Tap-Image) |
| 32 | 78.54 | 82.73 | -4.20 | 85.14 | -6.60 | 80.93 | -2.39 | 78.50 | 0.04 |
| 36 | 80.39 | 84.01 | -3.62 | 86.45 | -6.06 | 83.04 | -2.65 | 81.98 | -1.59 |
| 38 | 80.29 | 82.83 | -2.54 | 85.23 | -4.94 | 81.72 | -1.43 | 79.81 | 0.48 |
| 42 | 81.70 | 85.79 | -4.09 | 88.28 | -6.58 | 84.17 | -2.46 | 83.83 | -2.13 |
| 46 | 85.21 | 82.36 | 2.84 | 84.75 | 0.45 | 83.22 | 1.98 | 82.28 | 2.93 |
| 48 | 84.75 | 80.71 | 4.04 | 83.06 | 1.69 | 82.39 | 2.36 | 80.91 | 3.84 |
| 52 | 84.37 | 88.28 | -3.91 | 90.84 | -6.47 | 86.82 | -2.45 | 88.22 | -3.84 |
| 56 | 88.99 | 83.06 | 5.93 | 85.47 | 3.52 | 86.75 | 2.24 | 88.10 | 0.89 |
| 58 | 87.69 | 81.48 | 6.21 | 83.84 | 3.85 | 85.18 | 2.51 | 85.51 | 2.18 |
| 62 | 88.10 | 88.08 | 0.02 | 90.64 | -2.54 | 87.70 | 0.40 | 89.66 | -1.56 |
| 66 | 92.18 | 84.63 | 7.55 | 87.08 | 5.09 | 88.31 | 3.87 | 90.67 | 1.51 |
| 68 | 92.41 | 83.11 | 9.30 | 85.52 | 6.89 | 88.11 | 4.30 | 90.34 | 2.07 |
| 72 | 91.34 | 88.90 | 2.44 | 91.48 | -0.14 | 89.32 | 2.02 | 92.34 | -0.99 |
| 76 | 95.60 | 88.06 | 7.54 | 90.62 | 4.99 | 92.25 | 3.36 | 97.16 | -1.56 |
| 78 | 95.41 | 86.34 | 9.07 | 88.85 | 6.56 | 92.51 | 2.90 | 97.60 | -2.19 |
| RMS (Taps-Image) | | 5.51 | | 4.95 | | 2.65 | | 2.13 | |

References

¹Kavandi, J., Callis, J., Gouterman, M., Khalil, G., Wright, D., and Green, E., 1990, Lunimescent Barometry in Wind Tunnels", Review of Scientific Instruments, Vol. 61, No. 11, pp. 3340-3347.

² Morris, M.J., Donovan, J.F., Kegelman, J.T., Schwab, S.D., Levy, R.L., and Crites, R.C., "Aerodynamic Applications of Pressure Sensitive Paint", AIAA Journal, Vol. 31, No. 3, pp.419-425, 1993

³ McLachlin, B.G. and Bell, J.H., "Pressure Sensitive Paint in Aerodynamic Testing", Experimental Thermal and Fluid Science, 10, pp. 470-485, 1995

⁴ Liu, T., Campbell, B. T., Burns, S. P., and Sullivan, J. P., "Temperature- and Pressure-sensitive Luminescent Paints in Aerodynamics," Applied Mechanics Review, Vol. 50, No. 4, April 1997, pp. 227-246.

⁵ Oglesby , Upchurch, Pressure Sensitive Paint with Internal Temperature Sensing Luminophore, Proceedings of the 42nd International Instrumentation Symposium, 1996, pp 205-223

⁶ Schanze, K.S., Carroll, B.K., Korotkevitch, S., and Morris, M., Temperaure Dependence of Pressure Sensitive Paints, 1997, AIAA Journal, Vol.35, No. 2, pp306-310

⁷ Woodmansee, Methods for Treating Temperature-Sensitivity Effects of Pressure Sensitive Paints, 35th AIAA Aerospace Science Meeting , AIAA 97-0387

⁸ Taghavi, R.R., Raman, G., and Bencic, T.J., Mixer Ejector Wall Pressure and Temperature Measurements based on Photoluminescence, 1998 ASME Fluids Engineering Div. Summer Mtg, Paper No. FEDSM98-5085

⁹ Bencic, T.J., "Experiences Using Pressure Sensitive Paint in NASA Lewis Research Center Test Facilities", AIAA Paper 95-2831, 1995

¹⁰ Raman, G., Envira, E., Bencic, T.J., Tone Noise and Nearfield Pressure Produced by jet-cavity Interaction, NASA TM-1998-208836 (37th AIAA Aerospace Science Meeting, AIAA 99-0604)

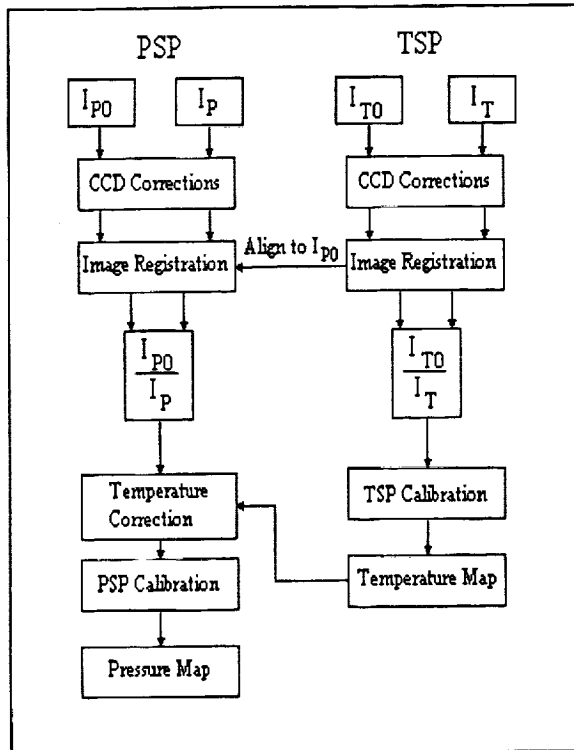


Figure 1. Flow diagram of data reduction procedure.

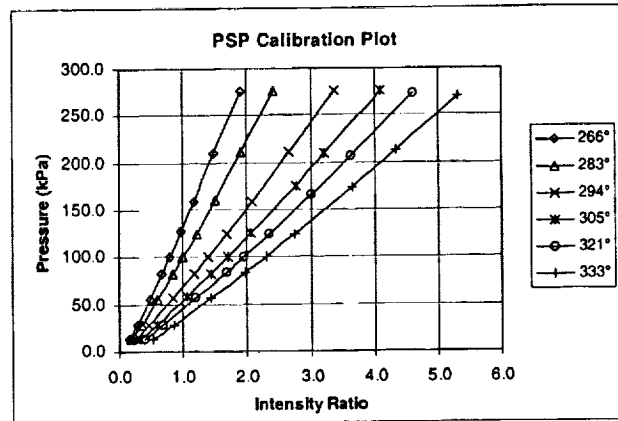


Figure 2. PSP calibration plot showing temperature dependence.

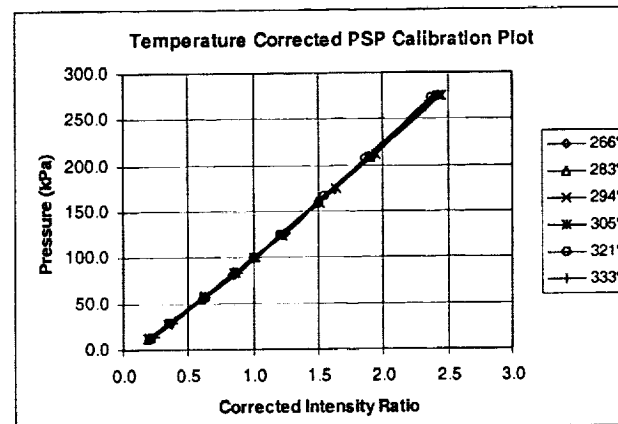


Figure 3. Temperature corrected intensity ratio data, all curves collapse on to one.

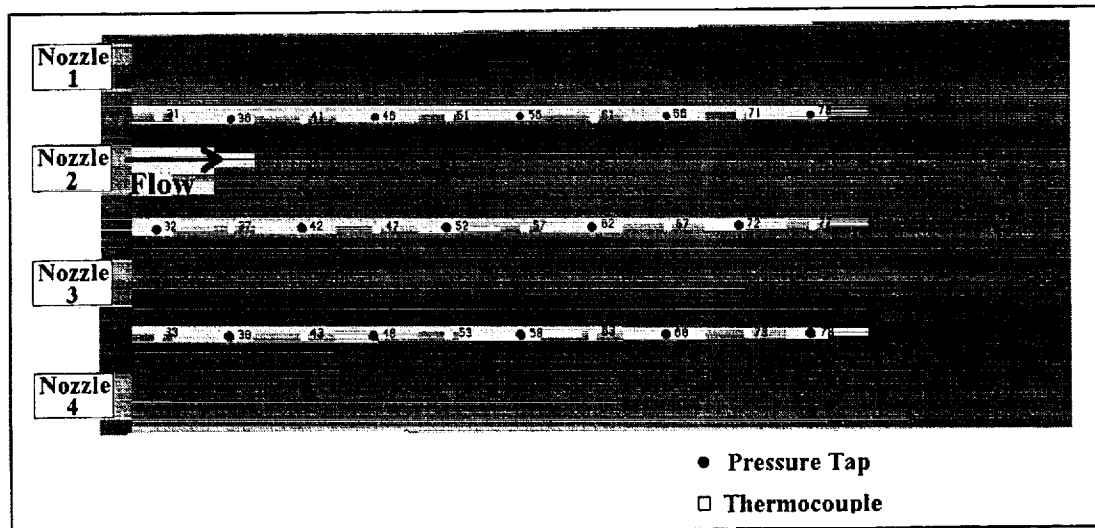


Figure 4. Instrumentation and nozzle location for supersonic multi-jet mixer ejector test.

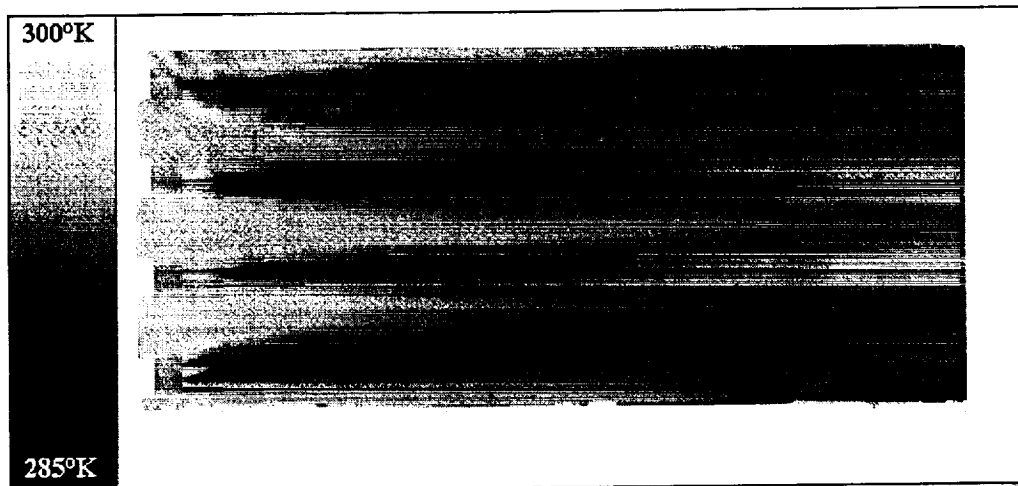


Figure 5. TSP temperature distribution of mixer-ejector acrylic surface.

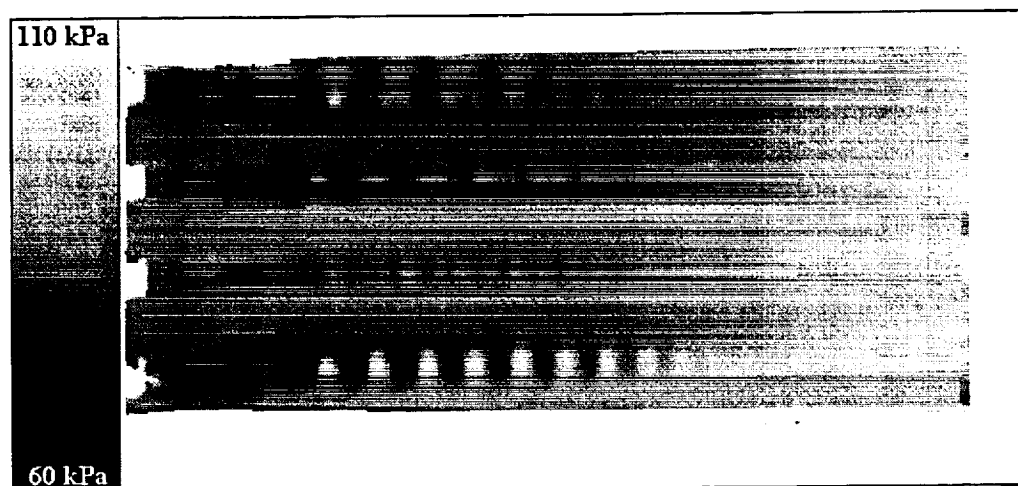


Figure 6. Non-temperature corrected PSP pressure distribution of mixer-ejector.

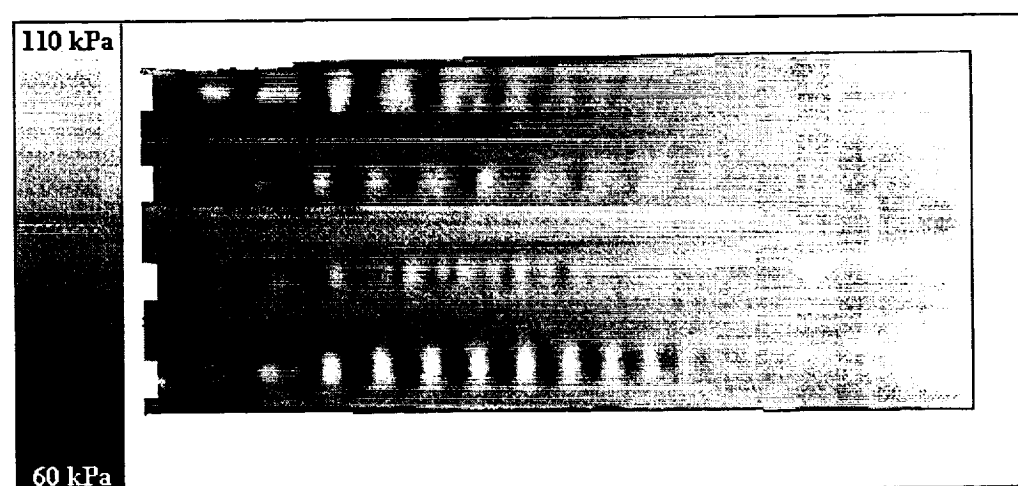


Figure 7. Temperature compensated PSP pressure distribution of mixer-ejector.

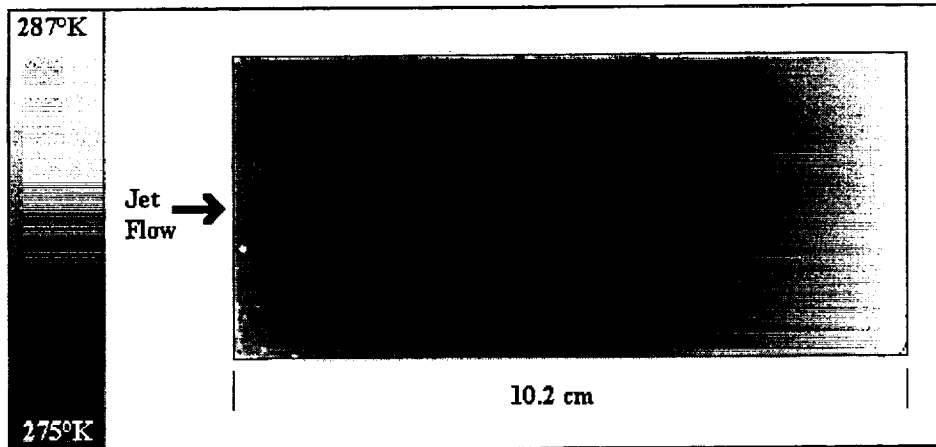


Figure 8. Temperature distribution of aluminum cavity floor with jet flow over the cavity.

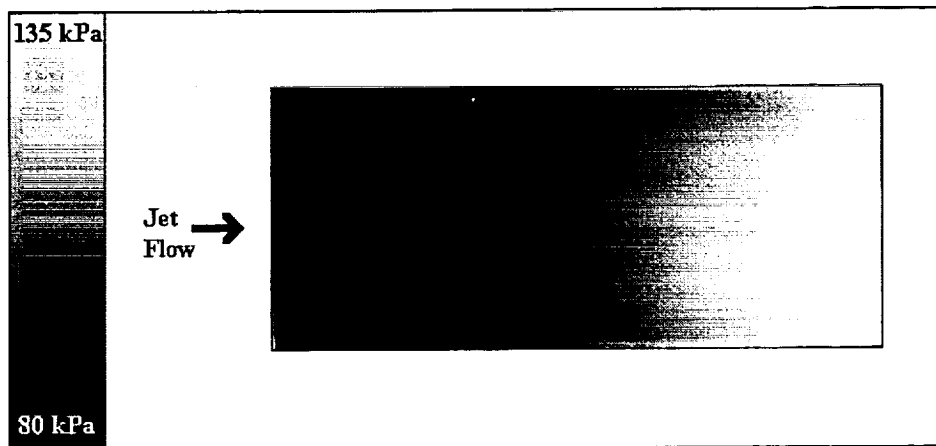


Figure 9. Pressure distribution of cavity floor with jet flow over the cavity.

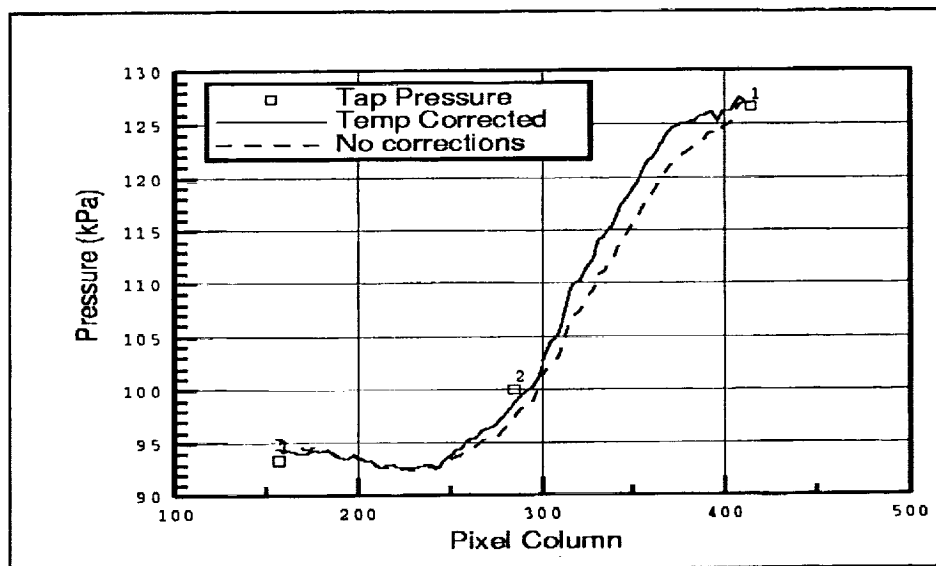


Figure 11. Plot of uncorrected and temperature compensated PSP data at cavity centerline.